

Use of four drought indices for evaluating drought characteristics under climate change in Shaanxi, China: 1951–2012

Rengui Jiang · Jiancang Xie · Hailong He · Jungang Luo · Jiwei Zhu

Received: 17 July 2014 / Accepted: 4 October 2014 / Published online: 12 October 2014
© Springer Science+Business Media Dordrecht 2014

Abstract Drought severity was simulated with four drought indices to examine the impacts of climate change on drought conditions in Shaanxi province over the period 1951 to 2012. The drought metrics analyzed were based on the original Palmer drought severity index (orPDSI), self-calibrated PDSI (scPDSI), the standardized precipitation index (SPI) and the standardized precipitation evapotranspiration index (SPEI). Both Thornthwaite (Thor) and Penman–Monteith (PM) parameterizations were used to calculate potential evapotranspiration (PET), and the differences between two PET estimators were studied. Nonparametric Mann–Kendall monotonic test was used to examine the trends of hydro-climatic data. Series of drought indices were compared at five meteorological stations with different climate characteristics, located in the north, central and south parts of Shaanxi province, respectively. Effects of climate change in drought conditions were investigated with hypothetical progressive precipitation decrease (−15 %) and temperature increase (2 °C). The results showed that there was discrepancy between PET estimated using the Thor and PM parameterization estimators, while the SPEI calculated with the two PET estimators are found to be similar. The SPEI has the combined advantages over the scPDSI and the SPI, considering the effect of temperature variability on drought severity and its multi-scalar characteristic, while scPDSI has an inherent approximately 12-month time scale. The Pearson’s correlation is used to compare the three pairs of drought indices combinations at different time scales. Under climate change conditions, the drought severity increases with the decline of precipitation and higher water demand as a result of the temperature increase based on the metrics of the scPDSI, the SPI and the SPEI.

Keywords Drought severity · Drought metrics · Extreme events · Potential evapotranspiration (PET)

R. Jiang (✉) · J. Xie · J. Luo · J. Zhu
State Key Laboratory Base of Eco-Hydraulic Engineering in Arid Area, Xi’an University of Technology, Xi’an 710048, Shaanxi, China
e-mail: jrengui@163.com

H. He
Department of Renewable Resources, University of Alberta, Edmonton, AB T6G2H1, Canada

1 Introduction

Drought can be considered as a period of water deficit for an extended period of time as a result of a deficiency in its water supply (e.g., atmospheric, surface or ground water; Dubrovsky et al. 2009) and is one of the most severe and frequently occurred natural hazards which have substantial impacts on economic, agricultural, ecological and environmental activity across the world (Begueria et al. 2010; Li et al. 2013; Vicente-Serrano et al. 2010a). The large spatial coverage and long-duration characteristics make it one of the most widespread and costliest natural disasters (Sheffield et al. 2009). The definition of drought has been one of the most important issues for drought detection, monitoring and analysis (McKee et al. 1993) because of its complex features (Vicente-Serrano 2007). Wilhite and Glantz (1985) clustered droughts into four types: meteorological, hydrologic, agricultural and socioeconomic droughts according to their delimiting criteria based on their leading causes and impacts. Drought severity can be measured according to its intensity and duration. Intensity represents the magnitudes of the drought indices, and duration can be identified by the onset and end of the drought episodes (Vicente-Serrano et al. 2010a). However, it is difficult to determine the onset, end and severity of the drought, which make it difficult to identify and quantify the effects of drought on economy, society and environment.

Many subjective indices have been proposed to quantify, monitor and analyze drought for the past twentieth century due to the difficulties in objectively identifying drought characteristics according to the intensity, duration and spatiotemporal patterns (Begueria et al. 2010; Vicente-Serrano et al. 2010a). Drought indices, such as Palmer drought severity index (PDSI) (Palmer 1965), crop moisture index (CMI) (Palmer 1968), drought area index (DAI) (Bhalme and Mooley 1980), standardized precipitation index (SPI) (McKee et al. 1993), standardized precipitation evapotranspiration index (SPEI) (Vicente-Serrano et al. 2010a), etc. (Li et al. 2013), have been frequently used to quantify drought severity (Table 1). However, those drought indices probably lead to some differences in values and change patterns, especially at relatively small scales, which are mainly caused by the availability and the resolution of the data set (Vicente-Serrano 2007; Vicente-Serrano et al. 2010a; Dai 2013). It is postulated that algorithm of drought indices with hydroclimatic variables such as precipitation, temperature and soil water-holding capacity should be helpful to drought analysis if we detect the main explanatory variable for drought indices. Further, research on the differences of drought indices should be useful to analyze drought severity (Wilhite and Glantz 1985; Vicente-Serrano et al. 2010a).

Climate of China shows a warm and dry trend and drought events occur more frequently because of the global warming, and this is much apparent during the past several decades (Cai et al. 2008). The long-term drought events in northern China starting 2000 and the severe drought in Yunnan province, southwestern of China in 2010, have caused devastating effects on regional agriculture, environment and socioeconomic (Qiu 2010; Sheffield et al. 2012). Several studies have investigated the drought in northern China over the past decade (Li et al. 2013; Xin-Gang et al. 2005; Zhao and Wu 2013; Zou et al. 2005). Zou et al. (2005) found the drought area in northern China had increased significantly since the late 1990s, the drought in 2000, for example, affected agricultural areas of up to 40 million hectares. At the meantime, unprecedented severe droughts took place in part of this region accompanied with severe economic losses such as Hebei and Shanxi provinces. However, few studies have analyzed the drought severity in Shaanxi province (northwestern China). This is probably due to the complexity in climates and landscapes in Shaanxi, which

Table 1 Several commonly used drought indices and references

Drought indices	References
Palmer drought severity index (PDSI)	Palmer (1965)
Crop moisture index (CMI)	Palmer (1968)
Drought area index (DAI)	Bhalme and Mooley (1980)
Standardized precipitation index (SPI)	McKee et al. (1993)
Vegetable health indices (VHIs)	Kogan (1997)
Self-calibrated PDSI (scPDSI)	Wells et al. (2004)
Standardized precipitation evapotranspiration index (SPEI)	Vicente-Serrano et al. (2010a, b)

consists of three main types of landscapes of different climates ranging from dry, cold desert in the north, mild plain in the middle, wet and warm mountains in the south. It provides us a great opportunity to investigate the drought severity and possible climate change impacts, which should be great beneficial to drought prevention and control in this region.

To provide a better understanding of different drought indices quantifying drought severity and possible climate change impacts on drought in Shaanxi province, four commonly used metrics of drought indices, Palmer drought indices including original PDSI (orPDSI) and self-calibrated PDSI (scPDSI), SPI and SPEI were selected to analyze the drought severity. Further, given that PET is one of inputs of drought indices, it is necessary to compare the results of PET based on different estimators since the PET values are not usually measured but estimated with empirical models (PET estimators). PET estimators result in different PET that may influence the calculation of drought index, but Droogers and Allen (2002) and Mavromatis (2007) showed that some of the drought index (e.g., PDSI) or different study areas may be insensitive to PET estimators. Therefore, it is necessary to test the impacts of different PET estimators on the drought predictions in Shaanxi. Climate change impacts on drought indices are investigated using hypothetical progressive precipitation decrease and temperature increase in this study. The results presented may provide more scientific support for drought detection, monitoring, prevention and control.

The primary objectives of this study are to: (1) compare the differences of two PET estimators and drought indices based on Thornthwaite (Thor) and Penman–Monteith (PM) parameterizations; (2) investigate the characteristics of drought severity as simulated by the orPDSI, scPDSI, SPI and SPEI; and (3) assess the sensitivity of climate change impacts using hypothetical progressive hydroclimatic changes on the drought severity.

The paper is organized as follows: A brief introduction of the study area and data are given in Sect. 2, two PET estimators and four metrics of drought indices are described in Sect. 2, results and discussion in Sect. 3, summary and conclusions in Sect. 4.

2 Materials and methodology

2.1 Study area and data

Shaanxi province, situated in the northwestern part of China, locates between 31.42°N–39.35°N latitude and 105.29°W–111.15°W longitude (Fig. 1). It homes to about



Fig. 1 Shaanxi province and the distribution of meteorological stations

205,800 km², and nearly 40 % is in the region of loess plateau (wind deposited, lack of vegetation cover and susceptible to wind and water erosion) that mostly lie in the north. Shaanxi province is divided into three parts according to the administrative zone, Shaanbei Plateau in the north, Guanzhong Plain in the central, and Qinling-Dabashan Mountains in the south. The landscapes range from windy desert region in the north to plain region in the central and mountain region in the south of Shaanxi province (Liu et al. 2013). The hydrological conditions of Shaanxi province are multifarious due to the diversity of its physiographic features and climate, which vary seasonally and regionally. The mean annual temperature is about 13 °C, nearly 10 °C in Shaanbei Plateau, 13 °C in Guanzhong Plain, 15 °C in Qinling-Dabashan Mountains, which decreases from southern to northern Shaanxi province. The mean annual precipitation is about 580 mm, most of which concentrates in the monsoon (May–October), nearly 400 mm, which also decreases from southern to northern. The altitude ranges from nearly 350 to 3,500 m, varied for different regions, with the mean altitude of approximately 1,127 m (<http://english.shaanxi.gov.cn>).

The monthly average precipitation and temperature for the period of 1951–2012 were extracted from the China National Climate Center (CNC) (available at <http://ncc.cma.gov.cn>), which have been under rigorous quality control and no filtering or modification were made for this study. The hydroclimatic data including precipitation and temperature are used to calculate the drought indices for five selected stations due to the availability of the long-term comprehensive data set and the climate features of Shaanxi province (Fig. 1), and those stations include Yulin and Yan'an in the Shaanbei Plateau, Xi'an in the Guanzhong Plain, Hanzhong and Ankang in the Qinling-Dabashan Mountains of Shaanxi province. The available water-holding capacity (AWC) of the soil at the selected stations used to drive the scPDSI was extracted from a global data set of water-holding capacity at the resolution of 1° (available at <http://daac.ornl.gov/SOILS/guides/Webb.html>), compiled by Webb et al. (2000). The data sets (wind speed, vapor pressure and cloud cover, expect precipitation, temperature) used to calculate the SPEI were obtained from the Climatic Research Unit (CRU) TS3 global data set (available at <http://badc.nerc.ac.uk/browse/badc/cru/data>) (Begueria et al. 2010).

2.2 PET estimators

Different methods have been used to estimate the PET from measured meteorological parameters (e.g., temperature, soil incoming radiation and heat fluxes). The commonly used methods are Thor parameterization (Thorntwaite 1948) and PM parameterization (Allen et al. 1998). The Thor parameterization only requires monthly average temperature and latitude of the station. This method is easily applicable, and the data are easily to be obtained. However, the PM parameterization method requires additional information such as wind speed, solar radiation and relative humidity, which are not usually available for majority of regions. The PM method is approved to provide better estimation of PET and has been adopted by several international organizations, such as the American Society of Civil Engineers (ASCE) and the Food and Agriculture Organization (FAO), to calculate PET.

The Thor parameterization of PET estimator for month i is given by Vicente-Serrano et al. (2010a),

$$PET_i = 16K_i(10T_i/I)^m \tag{1}$$

where T_i is the monthly average temperature ($^{\circ}\text{C}$). I is the heat index, computed as the sum of monthly index values from monthly average temperature,

$$I = \sum_{i=1}^{12} (T_i/5)^{1.514} \tag{2}$$

m is a coefficient based on heat index,

$$m = (6.75e07)I^3 - (7.71e05)I^2 + (1.79e02)I + 0.492 \tag{3}$$

K_i is a correction coefficient derived from the latitude and month i using the formula,

$$K_i = (n_{i1}/12) \times (n_{i2}/30) \tag{4}$$

n_{i2} in the formula is the number of days for the month i ; n_{i1} is the maximum number of sun hours for month i , which is compute by,

$$n_1 = (24/\pi) \times \arccos(-\tan \varphi \tan \delta) \tag{5}$$

where φ is the latitude of the station and δ_i is the solar declination using the formula,

$$\delta = 0.4093\text{sen}(2\pi J_i/365 - 1.405) \tag{6}$$

where J is the average Julian day of the month i .

The PM parameterization determines the PET using the rate of evapotranspiration from a hypothetical reference crop using assumed height of 0.12 m, a fixed surface resistance of 70 s/m and an albedo of 0.23 to represent the evapotranspiration of an united height of green grass surface that shade the ground totally, and with adequate water. The PM-based PET is calculated as follows (van der Schrier et al. 2011).

$$PET = \frac{0.408\Delta(R_n - G) + \gamma[900/(T + 273)]U_2(e_a - e_d)}{\Delta + \gamma(1 + 0.34U_2)} \tag{7}$$

where Δ and γ are the slope of vapor pressure curve and psychrometric constant ($\text{kPa}/^{\circ}\text{C}$); R_n and G are the net radiation of crop and the soil heat flux ($\text{MJ}/\text{m}^2\text{d}$); T and U_2 are the

average monthly temperature and the wind speed (m/s); $e_a - e_b$ represents the deficit of vapor pressure (kPa).

2.3 Drought indices

Four metrics of drought index, two Palmer drought indices including orPDSI and scPDSI, SPI, and SPEI are briefly introduced as follow.

1. Palmer drought indices (orPDSI and scPDSI)

The PDSI is computed based on the demand and supply of the water balance equation, which is a rather complex water budget system, using precipitation, temperature and soil characteristics (van der Schrier et al. 2011). It has a fixed 9- to 12-month temporal scale although it does not explicitly defined, and it does not consider different drought types (e.g., meteorological, hydrological and agricultural) (McKee et al. 1993; Vicente-Serrano et al. 2010b). The PDSI related the severity of drought to the accumulated weighted differences between actual precipitation and precipitation which are used to retain a normal water balance level (Wells et al. 2004), and different categories related to the PDSI values were identified to classify the dry and wet events (Palmer 1965). The orPDSI is probably the most widely used drought index in the USA and globally, which is commonly used to estimate the extended periods of abnormally dry or wet weather (Wilhite and Glantz 1985). However, it has several shortcomings, e.g., the effects of calibration period and areas used for calibration of parameters, lack of multiscalar characteristic, definition of PDSI values correlated to drought conditions, and spatial comparability (Vicente-Serrano et al. 2010a).

Because of the limited data and locations Palmer used to derive the weighting and calibration factors in the orPDSI algorithm, it is not comparable for diverse regions (van der Schrier et al. 2011). To address the deficiencies of the orPDSI, Wells et al. (2004) proposed a scPDSI algorithm that determined the factors using dynamically calculated values to replace empirical constants in the orPDSI algorithm for any location globally, which make PDSI values more homogeneous comparable and spatially, and represent extreme dry (wet) conditions better with frequencies (Vicente-Serrano et al. 2010a).

Following the Palmer's algorithm (Dai 2011; Palmer 1965; Wells et al. 2004), the moisture departure is represented by the difference between actual precipitation and supposed precipitation used to keep a normal soil moisture level in month i .

$$D_i = P_i - \hat{P}_i \quad (8)$$

$$\hat{P}_i = \alpha_i PE_i + \beta_i PR_i + \lambda_i PRO_i - \delta_i PL_i \quad (9)$$

where α_i , β_i , λ_i and δ_i indicate water balance coefficients i , which are calculated as follows:

$$\alpha_i = \overline{E_i} / \overline{PE_i}, \quad \beta_i = \overline{R_i} / \overline{PR_i}, \quad \lambda_i = \overline{RO_i} / \overline{PRO_i}, \quad \delta_i = \overline{L_i} / \overline{PL_i} \quad (10)$$

where E , R , RO , L represent evaporation, soils recharge, runoff and water loss of the soil layer, and the potential values of them are PE, PR, PRO, PL, respectively. Those variables rely heavily on the AWC of the soil. The overbar indicates the average value of those variables over the calibration period (1951–2011). The moisture anomaly index (Z index) for a given location and time period is compute as,

$$Z_i = D_i K_i \quad (11)$$

where K_i is the climatic characteristic coefficient, obtained by,

$$K_i = K_0 K'_i \tag{12}$$

$$K'_i = 1.5 \lg \left\{ \left[\frac{\overline{PE}_i + \overline{R}_i + \overline{RO}_i}{\overline{P}_i + \overline{L}_i} + 2.8 \right] / \overline{D}_i \right\} + 0.5 \tag{13}$$

The PDSI value X_i is computed using the weighted sum of the previous PDSI X_{i-1} and current moisture anomaly Z_i at given time i (Wells et al. 2004),

$$X_i = pX_{i-1} + qZ_i \tag{14}$$

where p and q are the duration factors, indicating the coefficients of sensitivity of PDSI to the Z index and autocorrelation of PDSI series. K_0 is the scaling factor.

Palmer (1965) calculated the duration factors using the data from Kansas and Iowa, and scaling factor using the data from nine locations in the central USA in the orPDSI algorithm, while the scPDSI determined the duration factors p and q and scaling factor K_0 based on the local climate conditions, more details see (Wells et al. 2004).

2. Standardized precipitation index (SPI)

The SPI considers the multiscalar characteristic of drought, which allows drought to monitor and analyze at different time scales (McKee et al. 1993). The procedure of SPI algorithm is as follows. Monthly precipitation P_i is used to calculate the SPI at the time scale of j months (e.g., 3, 6, 12 and 24 months). The SPI is then calculated using a Pearson III distribution and L-moment methods to get the probability distribution parameters (Vicente-Serrano et al. 2010a), which are then used to determine the intensity, duration and frequency of drought at given time scale. Different drought classifications are determined by different SPI values (Lloyd-Hughes and Saunders 2002; Patel et al. 2007), and drought is thought to start when the SPI falls below zero and end with positive SPI.

The calculation of SPI only needs precipitation, which is based on assumptions of dominant precipitation variability and stationary characteristic of other variables, such as temperature, evapotranspiration and wind speed (Vicente-Serrano et al. 2010b). Several previous studies indicated that precipitation is the dominant variable to determine the intensity and duration of drought. The simplicity and relatively less data demand make SPI widely used for drought analysis.

3. Standardized precipitation evapotranspiration index (SPEI)

The SPEI combines the advantages of simplicity of calculation procedure, multiscalar characteristic of SPI and considering the temperature variability of PDSI. It should be more suitable for drought detecting, monitoring and analysis, especially under the climate change scenarios. The calculation procedures of SPEI proposed by Vicente-Serrano et al. (2010a) are introduced as follows.

The monthly climatic water balance D_i of month i is computed using the difference between precipitation P_i and PET,

$$D_i = P_i - PET_i \tag{15}$$

Vicente-Serrano et al. (2010b) found a good fit between SPEI and the log-logistic distribution using the Kolmogorov–Smirnov test at all time scales globally. The three-parameter log-logistic distribution is used to calculate the SPEI based on the standardized D series, and it correlates well to the D series. The probability distribution function of the log-logistic distribution for D series is

$$F(x) = \left[1 + \left(\frac{\alpha}{x - \gamma} \right)^\beta \right]^{-1} \quad (16)$$

where α , β and γ are the scale, shape and origin parameters, respectively, which are obtained using the L-moment procedure (Vicente-Serrano et al. 2010a).

$$\begin{aligned} \beta &= \frac{2w_1 - w_0}{6w_1 - w_0 - 6w_2} \\ \alpha &= \frac{(w_0 - 2w_1)\beta}{\Gamma(1 + 1/\beta)\Gamma(1 - 1/\beta)} \\ \gamma &= w_0 - \alpha\Gamma\left(\frac{1+1}{\beta}\right)\Gamma\left(\frac{1-1}{\beta}\right) \end{aligned} \quad (17)$$

where $\Gamma(1 + 1/\beta)$ is the gamma function of $(1 + 1/\beta)$ and w_s is the probability-weighted moments (PWMs) of order s , $s = 0, 1, 2$.

$$w_s = \frac{1}{n} \sum_{i=1}^n \left(1 - \frac{j - 0.35}{n} \right)^s D_i \quad (18)$$

where n is the number of data points and j is the range of observations in increasing order.

SPEI is then calculated as the standardized values of $F(x)$ following the formula,

$$\text{SPEI} = W - \frac{2.515517 + 0.802853W + 0.010328W^2}{1 + 1.432788W + 0.189269W^2 + 0.001308W^3} \quad (19)$$

$W = \sqrt{-2 \ln(F(x))}$, when $F(x) < 0.5$, and $W = \sqrt{-2 \ln(1 - F(x))}$ when $F(x) \geq 0.5$.

SPEI value of 0 represents 50 % of the cumulative probability of D series.

2.4 Trend analysis

Nonparametric Mann–Kendall monotonic test was used for trend analysis of hydroclimatic data. To eliminate the influence of serial correlation on the trend detection of data series, the trend-free prewhitening (TFPW) approach proposed by Yue et al. (2002) was applied, but it essentially produced the same results (Gobena and Gan 2013). The trend magnitude is determined using Sen's slope β , defined as the median value of all possible combinations of pairs for the whole data set (Gan 1998; Yue et al. 2002).

$$\beta_k = \text{median}[(X_{jk} - X_{ik}) / (j - i)], \quad i, j \in [1, n] \quad (20)$$

where $X = \{x_1, \dots, x_i, \dots, x_n\}$, n is the length of X , k is the grid number, $i < j$. A positive (negative) value of β indicates an increasing (decreasing) trend.

3 Results and discussion

3.1 Estimate of PET

Taking Xi'an station, for example, Fig. 2a shows the annual accumulated values of PET using the PM parameterization and the Thor parameterization. The results show that the

PM-based PET is much higher than Thor-based PET. The underestimation of Thor-based PET should be correlated to the simplicity of the formulas (Eqs. 1–6), which is likely as a result of the exclusion of vapor pressure and cloud cover in the Thor-based PET algorithm. Both vapor pressure and cloud cover may cause more evaporation. The values of PET are assigned to zero using the Thor estimator, whereas PM-based PET can still be calculated when the temperature is below zero, which accounts for the higher values of PM-based PET than Thor-based PET (van der Schrier et al. 2011). On the other hand, the 12-month SPEI based on the two PET estimators is fairly similar in magnitude, as shown in Fig. 2b. Differences between SPEI_pm and SPEI_thor are also computed, and the results show that both SPEI_pm and SPEI_thor have higher values at certain periods (figure not shown). The correlation of 12-month SPEI is 0.9287 based on two PET estimators, higher than that of annual accumulated PET between the two parameterizations (0.8451).

Figure 2 indicates that the annual accumulated values of PET using two estimators have large differences, while the 12-month SPEI values are quite similar, which allows us to calculate the scPDSI and SPEI using the Thor-based PET estimator in the study. The results are generally consistent with previous studies. For example, Droogers and Allen (2002) found that the accuracy of PET mostly relies on the available and accuracy of meteorological data, and Vicente-Serrano et al. (2010a) indicated that the method for PET calculation is not critical to the drought index. Mavromatis (2007) revealed that the usage of different approaches to compute PET gets similar results when calculating the drought indices, such as SPI and PDSI. van der Schrier et al. (2011) investigated the sensitivity of the PDSI to both Thor-based and PM-based PET estimators. The results showed that annually accumulated PET varied in magnitudes, while the PDSI based on them was similar in regional average values, trends, correlation and extremely dry or wet events identification. Dai (2011) found that different PET algorithms have small influences on both the orPDSI and scPDSI during the twentieth century.

3.2 Current drought conditions

Software tools obtained from the GreenLeaf Project (available at <http://greenleaf.unl.edu/>) and SPEI R library (available at <http://sac.csic.es/spei/tools.html>) were used to calculate the drought indices (Vicente-Serrano et al. 2010b; Wells et al. 2004). The SPI and SPEI identify different types of drought at different time scales (ranging from 1 to 24 months), while the scPDSI has a single time scale. Drought is thought to be a multiscale phenomenon, and the multiscale characteristic of both SPI and SPEI makes it possible to analyze and monitor drought at different time scales (Vicente-Serrano et al. 2010a). The SPI and SPEI series show a short duration of negative value (drought) and positive value (wet) periods of high frequency at short time scales (e.g., 6 months). However, as the time period is lengthened to long time scales (e.g., 24 months), the periods with negative and positive values become in lower frequency but in longer duration.

Figure 3 is the evolution of the orPDSI, scPDSI, SPI and SPEI at different time scales (6, 12 and 24 months) for the period of 1951–2012 at Xi'an station. In general, orPDSI identifies more severe drought and wet events than scPDSI. Considering that orPDSI is calculated using the climatic characteristics based on the data from USA, scPDSI should be more accurate than orPDSI. Using four metrics of PDSI, Dai (2011) detected that the range of scPDSI values is slightly lower than orPDSI, and the self-calibrated climate characteristics make it more precise and comparable than orPDSI. According to the scPDSI, the most severe drought occurred in 1960, 1980, and in the decades of 1990 and 2000. These drought episodes are also identified by the SPI and SPEI at long time scale such as 12 and

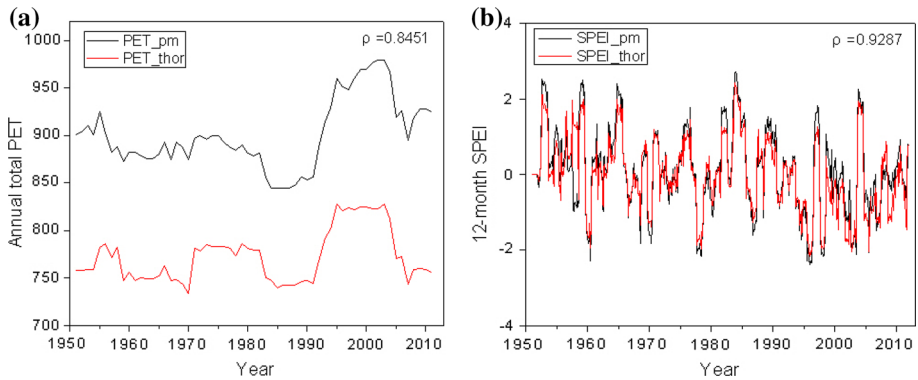


Fig. 2 Annual accumulated PET (**a**) of Xi'an station using the Penman–Monteith (*black line*) and Thornthwaite (*red line*) approaches. The correlation between PET_{pm} and PET_{thor} is 0.8451. The SPEI calculated with the Penman–Monteith-based (*black line*) and Thornthwaite-based (*red line*) PET. The correlation between SPEI_{pm} and SPEI_{thor} is 0.9287. Unit for PET is mm/year

24 months. The similar drought/wet periods identified by SPI and SPEI indicate the suitability to identify and monitor drought using SPI. However, apparent differences are also detected between scPDSI and SPI, and between SPI and SPEI series. Drought periods identified by scPDSI and SPEI in the decades of 2000 were not evident with the SPI series, especially at long time scales (24 months).

Table 2 shows the number of extreme ($|SPIs/SPEIs| \geq 2$, $lorPDSI/scPDSII \geq 4$) and moderate ($|SPIs/SPEIs| \geq 1$, $lorPDSI/scPDSII \geq 2$) drought/wet months between 1951 and 2012 at Xi'an station. To further investigate the drought/wet conditions at different decades, the period of 1951–2012 is divided into two parts: 1951–1981, and 1982–2012. Generally, for the period of 1951–2012, the total numbers of moderate drought/wet months for different drought indices at different time scales are almost identical, while the total number of extreme wet months is larger than that of extreme drought months. Both the total number and the number for each drought indices of extreme and moderate drought months tend to increase from the period of 1951–1981 to 1982–2012. Especially, all extreme drought months are detected between 1982 and 2012 for the scPDSI and SPEI series at time scales of 12 and 24 months. Comparing the orPDSI and scPDSI, it is evident that orPDSI identifies more extreme and moderate drought/wet months than scPDSI, which is also found in Fig. 3. The number of moderate drought identified by SPEI is larger than by SPI at all time scales, while the numbers of extreme drought identified by both SPEI and SPI are almost the same.

The results here generally concur with Dai et al. (1998), Zhao and Wu (2013), Zou et al. (2005). Dai et al. (1998) showed that drought risk and moisture surplus have been increased since the late 1970s as a result of global warming conditions. Zou et al. (2005) indicated that droughts have increased for the past several decades in some regions of northern China, especially after the late 1990s, and the drier climate in the northern China is mostly caused by less precipitation. Zhao and Wu (2013) found that the Loess Plateau experienced apparent increasing drought severity for the past several decades. According to the Bulletin of Flood and Drought Disasters in Shaanxi, more severe droughts are found after 1980s, such as 1998–2002, 2007 and 2011, which cause considerable economic losses. For example, the crops affected by the drought reached 20.82 million km², and the direct economic losses reached nearly 4.73 billion RMB in 2001 in Shaanxi province.

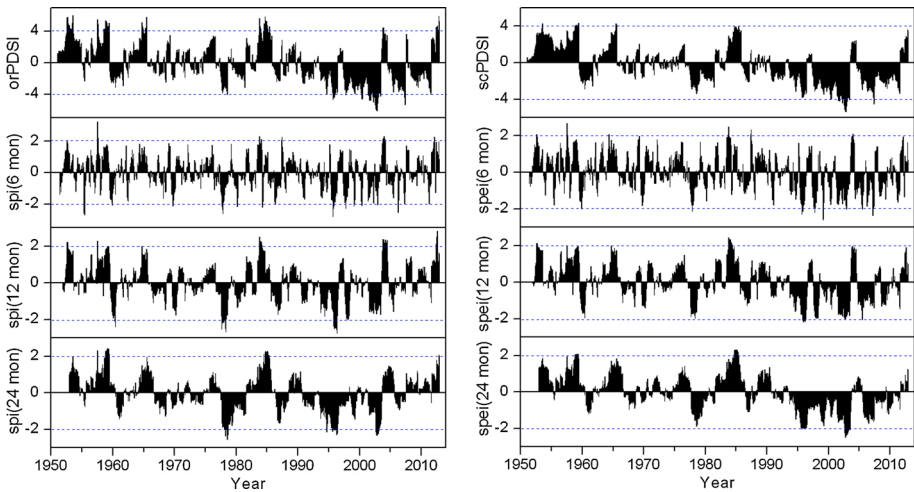


Fig. 3 Evolution of orPDSI, scPDSI, 6-, 12-, 24-month SPI and SPEI at the Xi'an station for the period of 1951–2012. The series above the dot lines represent extreme drought period (*negative values*) and extreme wet period (*positive values*)

3.3 Differences of drought indices

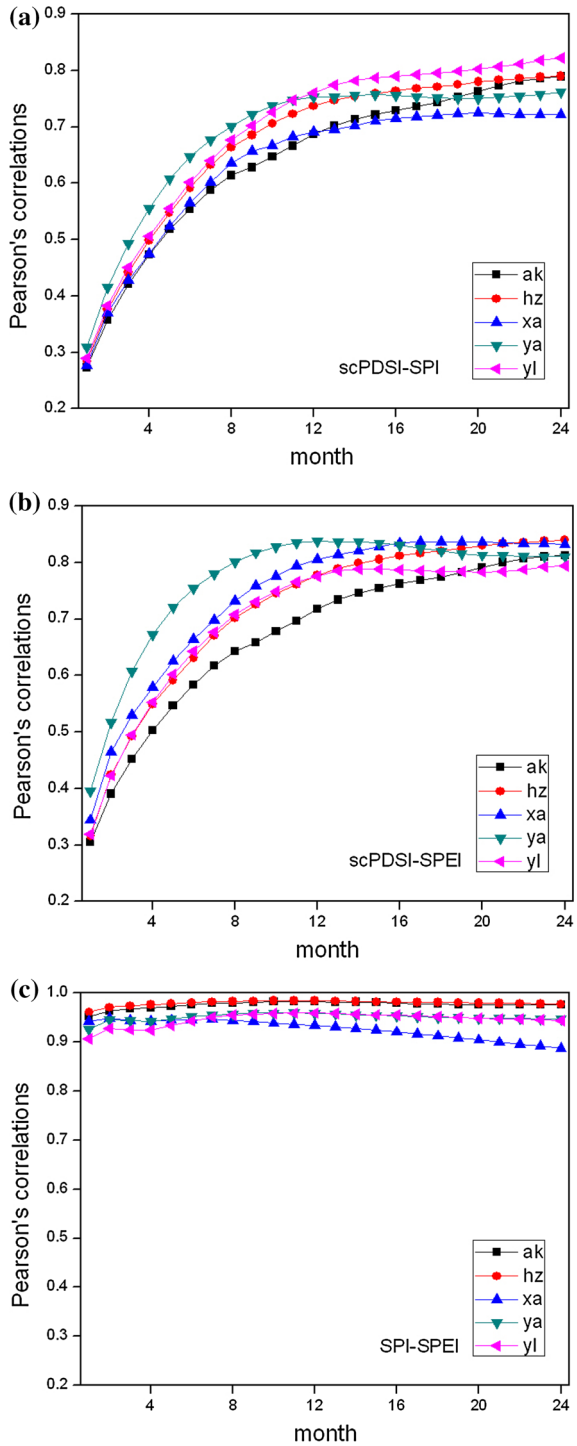
Figure 3 and Table 2 indicate that drought severity varies with four metrics of drought indices and also differs at different time scales of SPI and SPEI. Figure 4 shows the Pearson's correlations between the series of scPDSI and 1 to 24 months SPI and SPEI during 1951–2012 for five stations, as shown in Fig. 1. The scPDSI was highly correlated to SPI and SPEI between 12 and 24 months for all stations, with maximum values fluctuating between 0.65 and 0.85. The correlations between the scPDSI and the SPEI (Fig. 4b) were relatively higher than those between the scPDSI and the SPI (Fig. 4a). The correlations between the SPI and the SPEI were relatively high (0.80–0.98) at different time scales. However, the correlation decreased at longer time scales for Yulin, Yan'an and Xi'an stations, especially for Xi'an station (Fig. 4c). The correlations between orPDSI and scPDSI are between 0.94 and 0.98, which will not discuss further, since scPDSI is superior to orPDSI and more accurate for drought identification as explained in Sect. 3.2 (Wells et al. 2004).

Figure 4 indicates that the scPDSI exhibits similar drought severity with SPI and SPEI at time scale of approximate 12 months, which concurs with previous studies. For example, McKee et al. (1993) compared the Palmer drought index (PDI) with SPI and the results showed that the maximum correlation coefficient between PDI and SPI is 0.85, which is found at time scale of nearly 12 months, indicating that PDI has an inherent time scale. Lloyd-Hughes and Saunders (2002) found 12-month SPI is highly correlated to PDSI. Vicente-Serrano et al. (2010a) indicated that the PDSI has fixed temporal scales at 9–12 months, and the SPI exhibited close correspondence to the PDSI at 6- to 12-month time scales. The high correlation between the SPI and SPEI (Fig. 4c) shows that precipitation is the main explanatory variable to determine drought, especially for Ankang station, where the temperature change is stationary for the period of 1951–2012. However, differences between the SPI and SPEI are also detected over long time scales for Xi'an and Yulin stations where temperature has increased significantly during 1951–2012.

Table 2 Number of extreme and moderate drought/wet months for the periods of 1951–2012, 1951–1981 and 1982–2012 at Xi'an observation

Condition	Classification	Periods	Sp16	Sp12	Sp124	Spe16	Spe12	Spe124	OrPDSI	ScPDSI
Extremely wet	(SPIs/SPEIs ≥ 2 or orPDSI/scPDSI ≥ 4)	1951–2012	15	22	23	11	10	16	54	10
		1951–1981	3	3	11	4	2	6	32	10
		1982–2012	12	19	12	7	8	10	22	0
Moderately wet	(SPIs/SPEIs ≥ 1 or orPDSI/scPDSI ≥ 2)	1951–2012	119	116	120	127	126	117	165	120
		1951–1981	61	55	64	76	67	78	100	80
		1982–2012	58	61	56	51	59	39	65	40
Moderate drought	(SPIs/SPEIs ≤ -1 or orPDSI/scPDSI ≤ -2)	1951–2012	110	110	107	120	126	114	175	156
		1951–1981	41	38	39	31	33	27	31	27
		1982–2012	69	72	68	89	93	87	144	129
Extreme drought	(SPIs/SPEIs ≤ -2 or orPDSI/scPDSI ≤ -4)	1951–2012	18	17	20	11	9	14	30	14
		1951–1981	8	9	5	2	0	0	1	0
		1982–2012	10	8	15	9	9	14	29	14

Fig. 4 Pearson's correlations between the scPDSI, 1- to 24-month SPI and SPEI for the period of 1951–2012 at five stations: **a** scPDSI and SPI, **b** scPDSI and SPEI, and **c** SPI and SPEI



Using Sen's slope (Eq. 20), the trends of annual precipitation and annual temperature from 1951 to 2012 for five stations are investigated, as shown in Table 3. The results showed that annual precipitation in Ankang station has increased, while the annual precipitation in other four stations has decreased. All stations have increasing temperature trends, and four of which (except Ankang station) exhibited statistically significant increasing temperature trends at significant level of 5 %. To further examine the impacts of temperature on determining the drought severity, the differences in SPI and SPEI at 12- and 24-month time scales from 1951 to 2012 at both Xi'an and Ankang stations are computed, as shown in Fig. 5. In general, the results showed that the differences between the SPI and the SPEI were larger at Xi'an station than at Ankang station for both 12- and 24-month time scales. More negative values were found using the SPEI with respect to the SPI at Xi'an station, especially in the decade of 2000, while the differences between the SPI and the SPEI at Ankang station fluctuated slightly near zero. The results indicate that SPEI determines more drought severity due to the increasing temperature at Xi'an station. However, the inclusion of temperature in the SPEI algorithm does not provide much additional information at Ankang station, where temperature series are relatively stationary (Table 3). The results agree with the correlation analysis between the SPI and the SPEI (Fig. 4c), which reveal that the correlations between the 1- to 24-month SPI and the SPEI are much higher at Ankang station (0.95–0.98) than at Xi'an station (0.89–0.94). Vicente-Serrano et al. (2010a) also found that SPI exhibits little difference with scPDSI and SPEI when the temporal trends of temperature are inconspicuous.

3.4 Impacts of climate change

The Intergovernmental Panel on Climate Change Fourth Assessment Report (IPCC AR4) showed that the global average surface temperature has increased by 0.74 ± 0.18 °C over the last 100 year (1906–2005), and the warming rate has nearly doubled (0.13 °C \pm 0.03 °C per decade) over the last 50 years (1956–2005), than that of 1906–2005 (Jiang et al. 2014). In the meantime, the magnitude of precipitation decreased in some regions from 1900 to 2005. Global warming over the twenty-first century projected by the multi-scenario is similar to those observed for the past several decades (Pachauri and Reisinger 2008). Precipitation decrease and temperature increase under climate change have impacts on the intensity and duration of drought (Vicente-Serrano et al. 2010a). The results in Table 3 show that four out of five stations have decreasing precipitation and all the stations have increasing temperature trends under climate change for the past several decades (1951–2012). To investigate the potential impacts of climate change on drought conditions, hypothetical progressive precipitation decrease (–15 %) and temperature increase (2 °C) were used to calculate the modified drought indices series, according to the precipitation and temperature trends over the period 1951–2012, as shown in Table 2. For example, the temperature trend is 0.0311 °C/year at Xi'an station, which means the temperature has increased nearly 2 °C over the period 1951–2012.

Figure 6 shows the differences in scPDSI, the 12-month SPI and SPEI between the series of the original and modified series calculated based on a hypothetical precipitation decrease (–15 %) at Xi'an station. The results indicate that droughts increase in the intensity, duration and magnitude due to the hypothetical precipitation decrease for all drought indices, which especially evident for the SPI and the SPEI. For example, the modified drought severity represented using SPI tend to increase with respect to the original series of SPI over the period 1951–2012, especially after 1980. The SPI has relatively stable evolution and less difference in magnitude than the SPEI and the scPDSI. On the

Table 3 List of five selected meteorological stations in Shaanxi province, including station name, the World Meteorological Organization (WMO) number, location, characteristics of the annual precipitation and annual temperature

Station Name	WMO Number	Location		Annual precipitation			Annual temperature			
		Latitude (°N)	Longitude (°W)	Altitude (m)	Mean (mm)	Trend (mm/year)	Sig	Mean (°C)	Trend (°C/year)	Sig
Ankang	57245	32.72	109.03	562	819.08	0.9677	–	15.72	0.0051	–
Hanzhong	57127	33.07	107.03	614	865.52	–1.9811	–	14.52	0.0156	*
Xi'an	57036	34.3	108.93	400	580.89	–0.5600	–	13.81	0.0311	*
Yan'an	53845	36.6	109.5	991	533.24	–1.1951	–	9.86	0.0311	*
Yulin	53646	38.23	109.7	1131	402.69	–0.4167	–	8.4	0.0226	*

Sig represents statistically significant trend at significant level of 5 % (*)

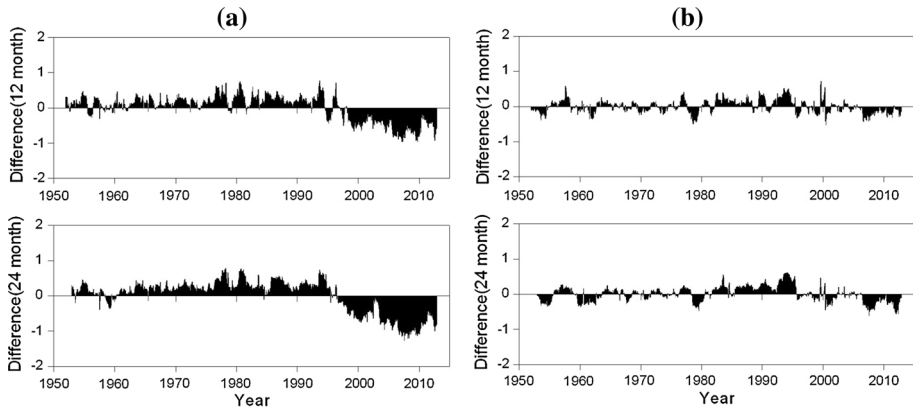


Fig. 5 Differences between 12- and 24-month SPI and SPEI during 1951–2012 at (a) Xi'an and (b) Ankang stations

other hand, Fig. 7 shows the differences in scPDSI, the 12-month SPI and SPEI between the series of the original and modified series calculated based on a hypothetical temperature increase (2°C) at Xi'an station. Again, the modified series of SPEI tend to decrease with respect to original series of SPEI over the period 1951–2012, especially after 2000, which indicates that the drought severity has increased. We do not calculate the modified SPI based on the temperature increase because it is a precipitation based drought index. The results show that drought severity has increased at the end of the century and early twenty-first century generally as a result of the hypothetical temperature increase.

Figures 6 and 7 are largely consistent with previous results, Dubrovsky et al. (2009) studied the impacts of climate change on drought conditions using PDSI and SPI. The results showed that drought risk increased when temperature increased based on the PDSI, and drought risk changed together with the precipitation based on the SPI. Vicente-Serrano et al. (2010a) found that the precipitation decrease and temperature increase had effects for drought conditions. Drought increased in intensity and duration with respect to the precipitation decrease and temperature increase.

4 Summary and conclusions

Four metrics of drought indices, including orPDSI, scPDSI, SPI and SPEI, were used to investigate the characteristics and possible climate change impacts on drought in Shaanxi province based on data from five weather stations over the period of 1951–2012. Our results are summarized as follows:

1. Thor and PM parameterization methods were selected to estimate PET which in turn was used as one of the inputs for orPDSI, scPDSI and SPEI. The results indicated that the annual accumulated PET estimators based on Thor and PM approaches result in different magnitudes, with correlation of 0.8451 (Fig. 2a), while the 12-month SPEI values using the two PET estimators are quite similar, with correlation of 0.9287 (Fig. 2b). Based on the orPDSI, scPDSI, SPI and SPEI, drought and wet conditions during 1951–2012 are identified and compared. The results show that the total number

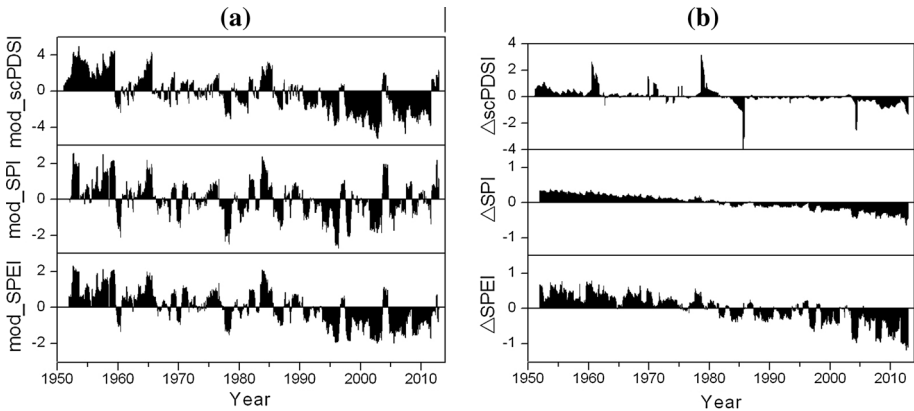


Fig. 6 Evolution of **a** modified series with hypothetical progressive precipitation decrease of 15 %, and **b** differences between original and modified series of scPDSI, 12-month SPI and SPEI for the period of 1951–2012 at Xi’an station

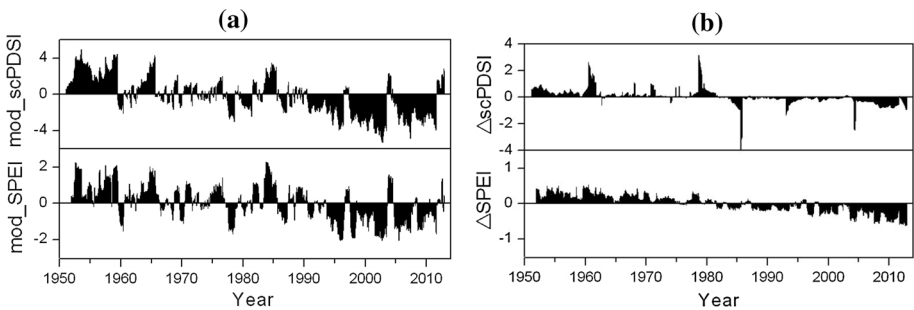


Fig. 7 Evolution of **a** modified series with hypothetical progressive temperature increase of 2 °C, and **b** differences between original and modified series of scPDSI, 12-month SPI and SPEI for the period of 1951–2012 at Xi’an station

of extreme drought months is less than that of extreme wet months for the period of 1982–2012. Both the total number and the number of extreme/moderate drought months tend to increase from 1951–1981 to 1982–2012 periods. The orPDSI identifies more extreme/moderate drought/wet months than the scPDSI, and the SPEI determines more drought than the SPI at all time scales. However, SPEI and SPI determine almost the same numbers of extreme drought.

2. The correlation analysis between the scPDSI, 1- to 24-month SPI and SPEI indicates that the scPDSI exhibits similar drought severity with SPI and SPEI at approximate 12-month time scale (Fig. 4a, b), indicating that the scPDSI has an inherent time scale at approximately 12 months, and the correction between scPDSI and SPEI is higher than that between scPDSI and SPI. The correlations between SPEI and SPI are detected relatively high at all time scales (Fig. 4c), which indicate that precipitation is the main explanatory variable of drought severity, while the correlations decrease after approximately 12-months time scale. However, differences exist at different stations, such as Xi’an and Ankang stations (Fig. 5), which are caused by the different

hydroclimatic characteristics of the stations. The SPEI does not provide additional information in comparison with the SPI when temperature of the station is relatively stationary, as detected at Ankang station (Table 3; Fig. 4c).

3. The impacts of climate change on drought are investigated based on the hypothetical progressive precipitation decrease (−15 %) and temperature increase (2 °C) according to the hydroclimatic trends for the period of 1951–2012. The results at Xi'an station indicate that the drought severity increases with the hypothetical progressive precipitation decrease (−15 %) for all the drought indices (Fig. 6b), especially for the SPI and SPEI. However, the SPI has relatively stable evolution and less difference in drought magnitude. The drought severity increases because of the hypothetical progressive increasing temperature (2 °C) are mainly detected at the end of the century and early twenty-first century (Fig. 7b).

Acknowledgments This work has been partly supported by the National Natural Science Foundation of China (Grant Nos. 51109175, 51109177 and 51209170), Research Foundation of State Key Laboratory Base of Eco-Hydraulic Engineering in Arid Area (Grant No. 2013ZZKT-5), Doctoral Start-up Foundation of Xi'an University of Technology (Grant No. 118-211413). The monthly hydroclimatic variables were provided by China National Climate Center (available at <http://ncc.cma.gov.cn>), and AWC data were obtained from Distributed Active Archive Center (DAAC) (available at <http://daac.ornl.gov/SOILS/guides/Webb.html>). The authors thank Drs. Thian Yew Gan, Santiago Beguería, Sergio M. Vicente-Serrano, and Xuezhi Tan for their assistance on this study. The comments of the anonymous reviewers have improved our manuscript.

References

- Allen RG, Pereira LS, Raes D, Smith M (1998) Crop evapotranspiration-guidelines for computing crop water requirements-FAO irrigation and drainage paper 56. FAO, Rome 300:6541
- Beguería S, Vicente-Serrano SM, Angulo-Martínez M (2010) A multiscalar global drought dataset: the SPEIBASE A new gridded product for the analysis of drought variability and impacts. *B Am Meteorol Soc* 91:1351–1354
- Bhalme HN, Mooley DA (1980) Large-scale droughts-floods and monsoon circulation. *Mon Weather Rev* 108:1197–1211
- Cai QF, Liu Y, Song HM, Sun JY (2008) Tree-ring-based reconstruction of the April to September mean temperature since 1826 AD for north-central Shaanxi Province, China. *Sci China Ser D* 51:1099–1106
- Dai AG (2011) Characteristics and trends in various forms of the Palmer drought severity index during 1900–2008. *J Geophys Res Atmos* 116:D12115
- Dai AG (2013) Increasing drought under global warming in observations and models. *Nat Clim Change* 3:52–58
- Dai A, Trenberth KE, Karl TR (1998) Global variations in droughts and wet spells: 1900–1995. *Geophys Res Lett* 25:3367–3370
- Droogers P, Allen RG (2002) Estimating reference evapotranspiration under inaccurate data conditions. *Irrig Drain Syst* 16:33–45
- Dubrovsky M, Svoboda MD, Trnka M, Hayes MJ, Wilhite DA, Zalud Z, Hlavinka P (2009) Application of relative drought indices in assessing climate-change impacts on drought conditions in Czechia. *Theor Appl Climatol* 96:155–171
- Gan TY (1998) Hydroclimatic trends and possible climatic warming in the Canadian Prairies. *Water Resour Res* 34:3009–3015
- Gobena AK, Gan TY (2013) Assessment of trends and possible climate change impacts in summer moisture availability in western Canada based on metrics of the Palmer drought severity index. *J Clim* 26:4583–4595
- Jiang R, Gan TY, Xie J, Wang N (2014) Spatiotemporal variability of Alberta's seasonal precipitation, their teleconnection with large-scale climate anomalies and sea surface temperature. *Int J Climatol* 34:2899–2917
- Kogan FN (1997) Global drought watch from space. *B Am Meteorol Soc* 78:621–636

- Li B, Su H, Chen F, Wu J, Qi J (2013) The changing characteristics of drought in China from 1982 to 2005. *Nat Hazards* 68:723–743
- Liu WL, Zhang MJ, Wang SJ, Wang BL, Li F, Che YJ (2013) Changes in precipitation extremes over Shaanxi province, northwestern China, during 1960–2011. *Quat Int* 313:118–129
- Lloyd-Hughes B, Saunders MA (2002) A drought climatology for Europe. *Int J Climatol* 22:1571–1592
- Mavromatis T (2007) Drought index evaluation for assessing future wheat production in Greece. *Int J Climatol* 27:911–924
- McKee TB, Doesken NJ, Kleist J (1993) The relationship of drought frequency and duration to time scales. In: *Proceedings of the 8th conference on applied climatology*, American Meteorological Society, Boston, MA 17(22):179–183
- Pachauri R, Reisinger A (eds) (2008) *Climate change 2007: synthesis report. Contribution of working groups I, II and III to the fourth assessment report of the intergovernmental panel on climate change*. Intergovernmental panel on climate change (IPCC): Geneva, Switzerland
- Palmer WC (1965) *Meteorological drought*. US Department of Commerce, Weather Bureau, Washington
- Palmer WC (1968) Keeping track of crop moisture conditions, nationwide: the new crop moisture index. *Weatherwise* 21(4):156–161
- Patel NR, Chopra P, Dadhwal VK (2007) Analyzing spatial patterns of meteorological drought using standardized precipitation index. *Meteorol Appl* 14:329–336
- Qiu J (2010) China drought highlights future climate threats. *Nature* 465:142–143
- Sheffield J, Andreadis KM, Wood EF, Lettenmaier DP (2009) Global and continental drought in the second half of the twentieth century: severity-area-duration analysis and temporal variability of large-scale events. *J Clim* 22:1962–1981
- Sheffield J, Wood EF, Roderick ML (2012) Little change in global drought over the past 60 years. *Nature* 491:435
- Thornthwaite CW (1948) An approach toward a rational classification of climate. *Geogr Rev* 38:55–94
- van der Schrier G, Jones PD, Briffa KR (2011) The sensitivity of the PDSI to the Thornthwaite and Penman-Monteith parameterizations for potential evapotranspiration. *J Geophys Res Atmos* 116:D03106
- Vicente-Serrano SM (2007) Evaluating the impact of drought using remote sensing in a Mediterranean, semi-arid region. *Nat Hazards* 40:173–208
- Vicente-Serrano SM, Begueria S, Lopez-Moreno JI (2010a) A multiscalar drought index sensitive to global warming: the standardized precipitation evapotranspiration index. *J Clim* 23:1696–1718
- Vicente-Serrano SM, Begueria S, Lopez-Moreno JI, Angulo M, El Kenawy A (2010b) A new global 0.5 degrees gridded dataset (1901–2006) of a multiscalar drought index: comparison with current drought index datasets based on the palmer drought severity index. *J Hydrometeorol* 11:1033–1043
- Webb RW, Rosenzweig CE, Levine ER (2000) Global soil texture and derived water-holding capacities (Webb et al.). Data set. available on-line [<http://www.daac.ornl.gov>] from Oak Ridge National Laboratory Distributed Active Archive Center, Oak Ridge, Tennessee, USA
- Wells N, Goddard S, Hayes MJ (2004) A self-calibrating Palmer drought severity index. *J Clim* 17:2335–2351
- Wilhite DA, Glantz MH (1985) Understanding: the drought phenomenon: the role of definitions. *Water Int* 10:111–120
- Xin-Gang D, Cong-Bin F, Ping W (2005) Interdecadal change of atmospheric stationary waves and North China drought. *Chin Phys* 14:850
- Yue S, Pilon P, Phinney B, Cavadias G (2002) The influence of autocorrelation on the ability to detect trend in hydrological series. *Hydrol Process* 16:1807–1829
- Zhao XN, Wu P (2013) Meteorological drought over the Chinese loess plateau: 1971–2010. *Nat Hazards* 67:951–961
- Zou X, Zhai P, Zhang Q (2005) Variations in droughts over China: 1951–2003. *Geophys Res Lett* 32:L04707